

Ice Detection Methods and Measurement of Atmospheric Icing

M. Wadham-Gagnon¹, N. Swytink-Binnema¹, D. Bolduc¹, K. Tété¹, C. Arbez¹

¹TechnoCentre éolien, Québec, Canada

mgagnon@eolien.qc.ca

Abstract: Accurate and reliable ice detection is essential for operators in the wind energy, aerospace, power transmission and transportation industries. Since these different operating conditions require different information about an event or site, it is useful to be able to directly compare multiple detectors under identical conditions.

This paper presents the results of a comparative study with 9 ice detection methods from a single test site in moderate icing conditions. These include three instrumental ice detection methods (a Combitech IceMonitor, double anemometry, and wind vane variation test), five meteorological ice detection methods (a horizontal visibility sensor, relative humidity sensor for dew point estimation, liquid water content from a Metek MRR, a Goodrich Ice Detector, and a Labkotech Ice Detector), and an ice accretion measurement from camera images.

The Goodrich and Labkotech produced good indications of meteorological icing while overestimating the duration compared to the methods based on horizontal visibility or liquid water content. The relative humidity method did not provide a good estimate of icing (indicating false positives more than 75% of the time). The Combitech provided instrumental icing estimations comparable to the double anemometry and wind vane variation methods with the added value of providing ice load measurements.

Images from a remote camera installed on the met mast, provide indisputable evidence of the presence (or not) of ice (provided there is good visibility of the structure being monitored). The image processing algorithm developed by the TechnoCentre éolien shows promising results for integration as an automated ice detection method.

Keywords: icing, ice detection sensors and methods, field study

LEGEND AND ABBREVIATIONS

AGL	Above Ground Level
CBH	Cloud Base Height measured from a ceilometer
HR	Horizontal Visibility
HUA	Heated Ultrasonic Anemometer
HV	Horizontal Visibility
LWC	Liquid Water Content
MRR	Micro Rain Radar
MVD	Median Volume Diameter
SNEEC	Site Nordique Expérimental en Éolien Corus
SR	Solar Radiation
T	Temperature
T_{dew}	Dew point temperature
TCE	TechnoCentre éolien
UCA	Unheated Cup Anemometer
WD	Wind Direction
WS	Wind Speed
WV	Wind Vane
σ	Standard deviation

INTRODUCTION

From power transmission to wind energy, ice detection methods provide total ice load, icing conditions, persistence, or other information depending on which limiting factor is most relevant [1].

Most detection methods provide an indication of meteorological icing, i.e. the period of active ice accretion, and/or instrumental icing, i.e. the period of time where ice is present on a structure or instrument. Few sensors or methods provide information regarding severity (ice load) or intensity (icing rate).

In the wind energy industry, some turbines may be equipped with ice protection systems while others may have preventive shut down strategies during icing events [2], [3]. Both strategies attempt to reduce icing-related production losses and both could greatly benefit from reliable ice detection.

A previous study, conducted in moderate to severe icing conditions in Sweden, compared the IceMonitor, Goodrich, Labkotech, and Holooptics ice detectors with a camera and heated/unheated anemometer measurements [4]. The intent of the present paper is to extend the comparative analysis to tests based on dedicated ice detectors, standard meteorological instruments, and novel detection methods during light to moderate icing conditions.

I. SITE, SENSORS AND METHODS

In order to compare the performance of different ice detection methods, a measurement campaign was conducted by TechnoCentre éolien (TCE) using sensors installed at the Site Nordique Expérimental Éolien Corus (SNEEC). The measurement campaign was conducted on a 126 m meteorological mast at the SNEEC test site, based in Rivière-au-Renard, Québec, Canada.

The sensors and methods discussed in this paper are described in Table 1. Each method will be referred to hereinafter by the acronym/abbreviation defined in this table. All methods are intended to detect ice at 80m above ground level which represents the hub height of the wind turbines installed on the same site.

The criteria used to determine the presence of ice for each method are provided in Table 2.

The LID, GID and CIM methods are based on simple criteria defined to interpret the signal of the specialised ice detection sensors. Note, however, that the thickness measured by the GID is in fact a pre-set linear calibration based on a vibration frequency; it was not calibrated after installation.

The RHT, WDD and WSD methods are based on standard data quality control tests [8].

The CAM method in the context of this study consists of analysing images taken from a camera installed on the meteorological mast. The thickness of ice is measured on the vertical section of the boom that supports an anemometer using an automatic image analysis algorithm developed by TCE.

Table 1: Description of ice detection methods

Method	Sensor	Description
CAM	Camera	Ice thickness measured from images of vertical anemometer support
CIM	Combitech Ice Monitor	Freely rotating ISO cylinder with load sensor [5]
GID	Goodrich 0872F1	Specialised ice detection sensor based on ultrasonic frequency change [6]
HVT	HV, T	Based on Horizontal Visibility and Temperature criteria
LID	Labkotec LID-3300IP	Specialised ice detection sensor based on ultrasonic frequency change [7]
LWCT	MRR & T	Atmospheric icing based on LWC measured from MRR and T
RHT	RH, T	Based on relative humidity and temperature criteria
WDD	WV	Detects ice from the variation in standard deviation of WD
WSD	HUA, UCA	WS difference between HUA and UCA

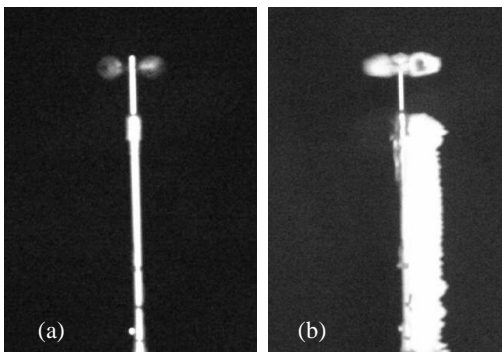
Table 2: Ice detection criteria for the different methods

Method	Icing Criteria
CAM	N/A
CIM	Load > 0.2 kg/m
GID	Thickness > 1 mm
HVT	HV < 300m T < 1°C
LID	Signal < 60% within past 30 min
LWCT	LWC > 0.1g/m ³ at 75m AGL T < 0°C WS > 4 m/s
RHT ¹	T - 0.9T _{dew} < 1°C T < 1°C
WDD	$\sigma_{wv} < 3^\circ$ Or: $\sigma_{wv} < 1/3 \sigma_{wv(ref)}$ T < 1°C
WSD	$(WS_{HUA} - WS_{UCA}) / WS_{HUA} < 80\%$ WS _{HUA} > 4 m/s T < 0°C

1. T_{dew} is calculated with the Magnus-Tetens equation [9], which is a function of relative humidity.

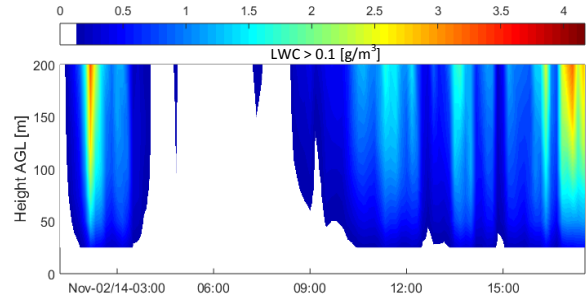
The camera images were recorded every 10 minutes at low resolution as they were initially not intended to be used for ice detection by image analysis. An example of non-iced and iced anemometer and vertical support structure is given in Figure 1.

As the direction of ice accretion on the anemometer's boom depends on the wind direction, the image analysis algorithm may not measure the maximum thickness of ice on the structure. Due to this, the measured ice thickness was an estimate provided for qualitative purposes only in the present study; no ice detection criterion was associated. For the same reason, the ice load, which may be estimated using ISO 12494 [10], was not calculated.

**Figure 1: CAM image of (a) a non-iced anemometer, and (b) an iced anemometer and shaft**

The HVT method is based on the horizontal visibility as measured by a CS120 visibility sensor at 18 m AGL.

Finally, the LWCT method uses LWC measured from a Metek Micro Rain Radar (MRR) installed next to the met mast. An example of LWC measurement is shown in Figure 2. This method detects ice when LWC greater than 0.1g/m³ is measured at 75m above ground level and temperature measured at the same level (from a thermometer on the met mast) is below 0°C. Note that the MRR measures precipitating water content but not cloud water content. This is due to the water droplet diameter range it is capable of registering. Hence, this method was used as a preliminary test of the potential of the equipment.

**Figure 2: Sample LWC time series measured from an MRR sensor between 25 m and 200 m above ground**

II. ICING DURATION

A. Annual Statistics

Total icing duration over the winter 2014-2015 months is shown in Figure 3, with each method identified as indicating either meteorological (met) or instrumental (ins) icing. The GID and LID methods estimate durations of meteorological icing close to the durations of instrumental icing estimated by the CIM, WSD and WDD. This is unexpected as the instrumental-to-meteorological icing ratio on this site has previously been observed to be of the order of 2 to 1 [11]. The HVT method for meteorological icing compared to the CIM or WSD methods for instrumental icing are closer to reflecting this ratio. It is noted that the LID method relies on a criteria that is based on the heating cycle of the sensor (30-40 minutes). The heating cycle of the sensor may cause this method to overestimate meteorological icing. Meanwhile the GID method tests whether a single point has surpassed its threshold. While this has a more rapid response time, a low threshold may be too sensitive while a high threshold results in numerous “on-off” cycles within a single event. For the present analysis, a low threshold was used, which may explain the higher-than-expected hour count. Further investigation is required.

The duration of meteorological icing based on the RHT method is at least 4 times greater than any other method (instrumental icing included). This suggests that the RHT method is false-positive at least 75% of the time, supporting earlier reports that the method is unreliable [12].

The CIM and WSD methods estimate just over 400 instrumental icing hours each. The HVT method indicates the lowest number of meteorological icing hours yet is within the expected ratio compared to instrumental icing of the CIM and WSD methods.

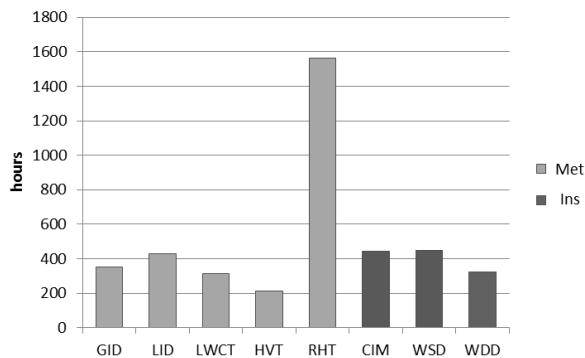


Figure 3: Duration of icing detected by different methods over the course of winter 2014–2015 (Nov to Apr)

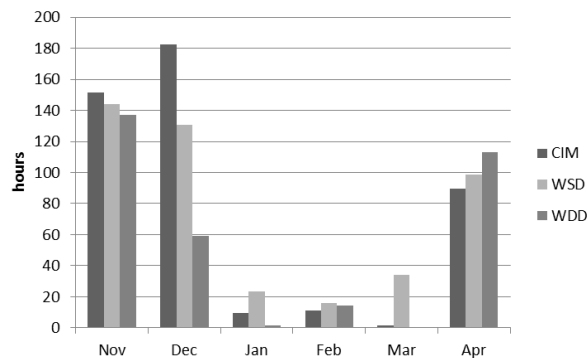


Figure 5: Monthly duration of instrumental icing detected by different methods during winter 2014–2015

B. Monthly Statistics

The number of hours of icing per month is shown in Figure 4 for methods intended to detect meteorological icing and in Figure 5 for methods intended to detect instrumental icing. Figure 4 illustrates how the RHT method greatly exceeds all other method estimations in every month. The other methods are comparable with the exception of the months of January when the HVT method suggested almost no icing hours, and February when both the GID and HVT methods suggested almost no icing hours.

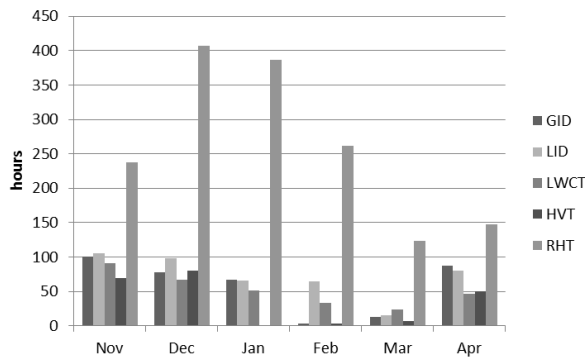


Figure 4: Monthly duration of meteorological icing detected by different methods during winter 2014–2015

The methods intended to detect instrumental icing are in good agreement in November, February, and April (Figure 5). The large difference between the methods in December is likely due to the low wind speeds during the main icing event of that month (see the following section). WSD excludes possible false positives at low wind speeds when cup anemometers underestimate the wind speed. Similarly for WDD, readings at low winds are unreliable due to the cut-in speed of the wind vane. Periods of low winds were therefore excluded from the analysis yielding a significantly lower icing duration than the other instrumental methods in December.

III. ICING EVENTS OF INTEREST

Of 20 icing events identified based on the GID method during the winter, three are presented in this paper.

A. Event 1 (Nov 2-5, 2014)

The first event (Figure 6) is a “text book example” with all sensors and methods (except RHT) working as expected. Active ice accretion in the beginning observed with CAM coincides with a higher frequency of heating cycles with the GID method. The raw LID data may be seen to decrease below its heating threshold (60% signal level) implying that ice was still accumulating at least one sampling period – 30 s – after it started heating.

Inspection of the CAM images reveals that ice was shed from part of the support around 22:40 on Nov 2. The anemometer itself remained iced, however, as is also confirmed by WSD (which uses different anemometers). The camera lens was covered in ice for a period, preventing good CAM data. Ice was then shed along the same section of the support around 18:00 on Nov 3 but remained on the anemometer rotor until the temperature had risen above 0°C around 6:40 Nov 5.

The WSD and WDD returned to the non-iced condition when the temperature rose. In contrast, the CIM took 6 hours longer. Since the anemometer did not completely freeze during the event, slightly higher vibrations and relative wind vectors may have quickened the ice shed compared with the static CIM sensor.

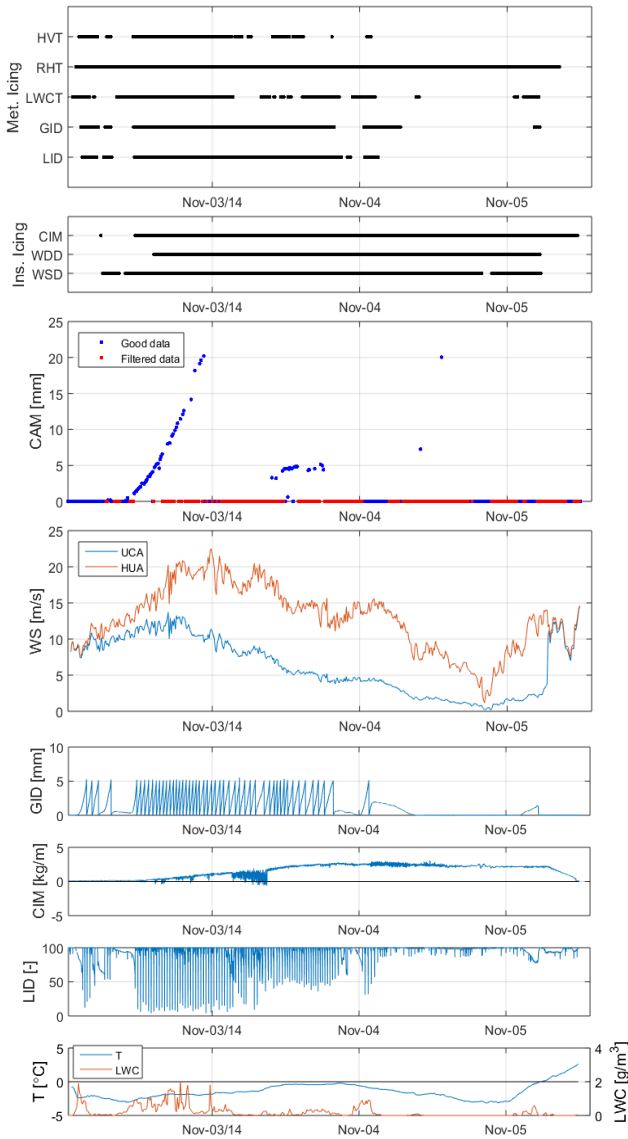


Figure 6: Ice detection methods and raw data – Event 1

B. Event 2 (Dec 17-25, 2014)

The second event, seen in Figure 7, lasted over 7 days with a single day of meteorological icing. Once again, the meteorological methods coincide with CAM accretion, though they have some offset in their start and finish times. The LID algorithm requires that a heating cycle is initiated and so is less sensitive than a visual inspection of the raw data would suggest – LID therefore appears later than GID despite both raw data time series showing signs of ice at the same time. GID stopped indicating ice the first time it reached its heating threshold because further ice accretion was not sufficient to attain its icing threshold after that point. In contrast, LID raw data suggest that a strong icing event continued after GID and CAM indicate no additional accretion. This behaviour for the LID sensor was observed at other instances during the winter when observations indicated very minimal ice accretion, and may be caused by non-icing precipitations.

CIM, CAM, and WSD raw data indicate a five-day period of instrumental icing which is not fully accounted for by the WSD and WDD methods. This is likely caused by each method's threshold criteria. The WSD method requires winds above 4 m/s measured by the HUA to prevent false positives. It is also likely that the standard deviation criteria of the WDD

method are not met at low wind speeds but this needs to be verified.

On Dec 24, freezing rain appears to have caused a short event and some ice accretion though it is uncertain why the CAM method did not measure it as the images were reasonably clear.

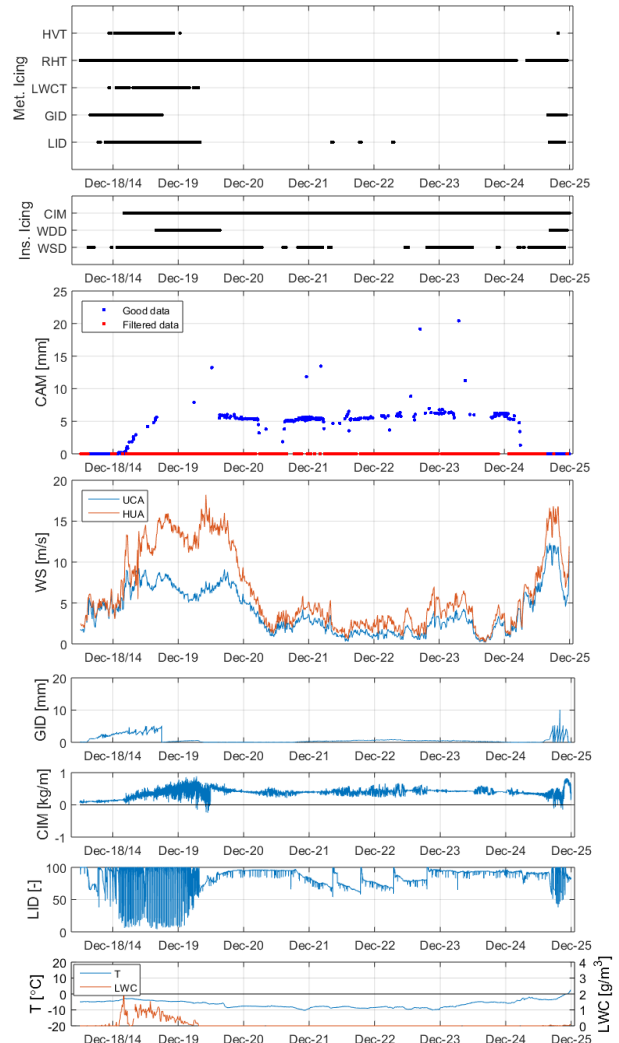


Figure 7: Ice detection methods and raw data – Event 2

C. Event 3 (Apr 21-27, 2015)

Event 3, a 4-day icing event shown in Figure 8, began in higher winds than the previous two but the winds decreased as the event intensified (seen in the higher cycle frequency of the GID raw data); this may have caused the UCA to freeze completely in early morning Apr 22. Ice accreted intermittently for the remainder of the event, though once again the LID raw data indicated a much more severe event than the GID in the latter half.

The instrumental icing methods indicate similar trends to one another except the CIM start time, which is approximately 12 hours behind the WDD and WSD methods. The raw CIM data indicates a negative load during this time; this is an occasional issue which tends to occur at the beginning of icing events. Note that the noise in the raw CIM data in Figure 8 is significantly reduced compared with the first two events because 10 minute average data acquisition was implemented in March 2015 in place of the 30 s single samples taken before.

There is a significant difference between the meteorological icing methods for this event. The GID suggests ice is accreting during the majority of the event. The raw GID data suggest that

ice accretion was slow or even reversed during some of the time; this behaviour is not accounted for by the single threshold which assumes a positive ice accretion *rate* above a 1 mm ice accretion signal level. In contrast, the LID method matches its raw signal more closely. Whereas the GID method uses a threshold based on a single point, the LID method requires the threshold to be passed at some point in the previous 30 minutes (about the time of a heating cycle during an icing event).

In early morning Apr 26, a small event with temperatures at or just above 0°C and no measured LWC caused the UCA to freeze again soon after its ice was shed. During the previous period, however, all methods correctly indicated an absence of ice formation conditions.

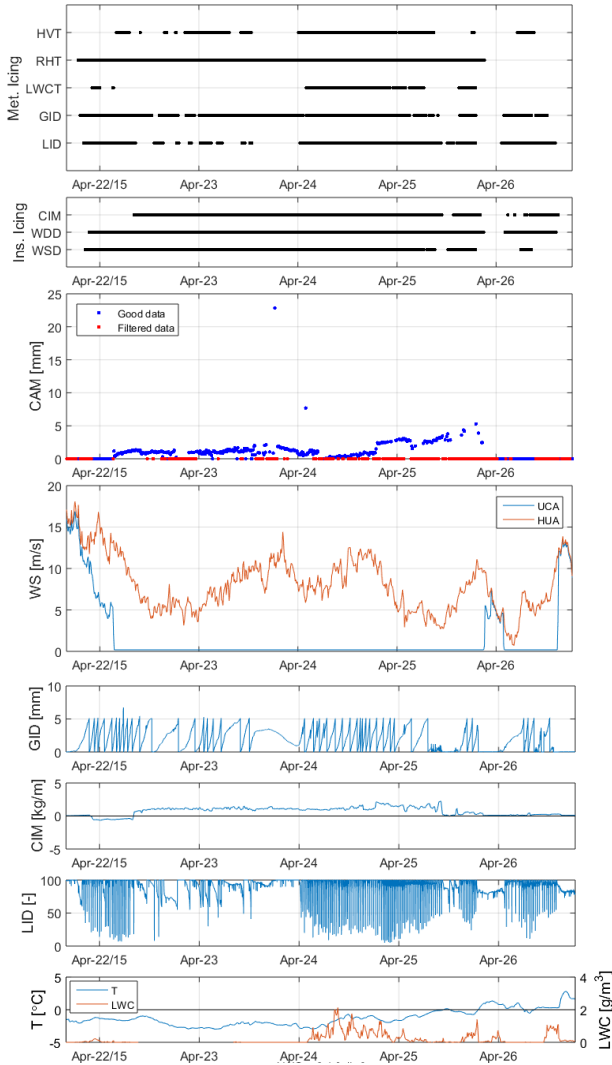


Figure 8: Ice detection methods and raw data – Event 3

IV. ICING SEVERITY

Icing severity may be interpreted through further processing of several of the methods presented. A quantitative analysis will be presented in a future paper, but some discussion is included here by way of introduction.

Heating cycle frequency may be counted with cyclically-heated ice detectors such as the LID and GID. Higher frequencies therefore indicate more severe icing. In Event 3, for example, the GID heating cycle which begins at midnight Apr 26 lasts 6 hours whereas the one immediately following lasts one hour, thereby suggesting a six-fold increase in severity. Both the GID and LID detectors have adjustable parameters which would enable shorter heating cycle times: the current 30 min or greater cycles are not conducive to (wind)

industry-standard 10 min averaging. Using the GID raw data, the events may be classified in order of most to least severe as: Event 1, 3, and 2.

Using accumulating instrumental icing methods, such as CAM and CIM, the icing severity may be estimated based on the total accretion, either in mm (camera), kg/m (CIM), or by converting to a standard ice class using Annex A of [10]. With these methods, the derivative of the data yields the accretion rate. As discussed previously regarding Figure 7, the CAM method (and CIM) may indicate both the meteorological and instrumental icing in this way. The CIM suggests that, in terms of total ice accretion, Event 1 was most severe, followed by Event 3 and Event 2. Icing severity could not be estimated from the CAM method as implemented in this setup: as discussed in Section I, the maximum ice thickness was not measured.

Finally, the LWCT method may be extended into an ice accretion model using WS, LWC, and T [10]. This would estimate the ice load (kg/m) or accretion (mm) during an icing event on a standard reference tube.

V. CONCLUSION AND FUTURE WORK

A comprehensive study of 9 ice detection methods was presented for a single test site in Québec, Canada over the winter 2014–2015. It has provided a means of direct comparison between methods overall (icing hours) and for specific events (sensitivity of each instrument from beginning of accretion to ice shed). The following conclusions could be drawn:

- The LID method shows ice accretion after the heating cycle is initiated providing an indication of icing intensity.
- The GID method also provides an indication of icing intensity as the sensor increases the frequency of heating cycles during periods of active ice accretion.
- The HVT method followed the LID quite closely for all three events, but reported half the total icing hours. HVT may be the more accurate measurement of the two since the LID method was found to overestimate ice accretion during small icing events.
- The RHT method provides excessive false positive results.
- The CAM method provides the most information on the icing event but relies on the camera lens not being obstructed by ice. This can be managed with adequate heating and protection from ice. The algorithm also relies on the quality of the images and may not be capable of detecting ice when there are not sufficient contrasts in the images.
- The WSD and WDD methods provide reliable indication of instrumental icing but may need to be refined for low wind speeds.
- With 10 minute averaging, the CIM method yielded a consistent instrumental icing response though its load measurement was not validated and it occasionally reported negative load values.
- The LWCT method followed meteorological icing of other methods, but is incomplete as it does not capture in-cloud icing. Its suitability for ice detection and forecasting needs to be investigated further.
- The LID and GID methods measured a high number of meteorological icing hours relative to instrumental icing hours measured with WSD and WDD methods. Further investigation is warranted.

Many of the sensors used in this analysis were installed in 2014 and have only experienced a single (relatively mild) winter. The researchers plan to continue the study into the winter 2015–2016 in the hopes of increasing the number and severity of observed icing events.

An ice accretion model based on LWC, WS and T may be developed and algorithms for ice severity based on the LID and GID methods may be completed in the future.

As well, ice detection based on cloud base height and temperature has shown promising results in previous studies. Data from a ceilometer sensor is available and will be included in a future paper.

ACKNOWLEDGMENT

The authors would like to thank their colleague Charles Godreau for running the image analysis for the CAM method. TCE operations and the SNEEC wind farm infrastructure are made possible with the support of the Québec Government's "Ministère Finance et Économie" and Canada Economic Development. The met mast was installed with funding from the Canada Foundation for Innovation, Renewable NRG Systems and RES Canada. Finally, the TCE mandate as a college centre for technology transfer in wind energy is provided by the "Cégep de la Gaspésie et les Îles".

REFERENCES

- [1] S. Fikke, et al., "COST 727: Atmospheric Icing on Structures Measurements and data collection on icing: State of the Art", Publication of MeteoSwiss, 2006
- [2] J. Nelson, "L'expérience de TransAlta avec le givrage des pales", 6th Quebec Wind Energy Conference, Carleton-sur-mer, 2012
- [3] S. Trudel, "Les arrêts préventifs: solution face au givre", 8th Quebec Wind Energy Conference, Gaspé, 2014
- [4] H. Wickman, et al., "Experiences of different ice measurement methods," Elforsk Report 13:15, 2013
- [5] Combitech, "The Ice Load Surveillance Sensor IceMonitorTM", Product Sheet, 2013
- [6] Campbell Scientific (Canada) Corp., "0872F1 Ice Detector Instruction Manual", 2014
- [7] Labkotec Indutrade Group, "LID-3300IP Ice Detector - Installation and Operating Instructions", 2014
- [8] TechnoCentre Éolien, "PRO-REC 002: Procédure de contrôle qualité des données", Gaspé (Québec) Canada, 2014.
- [9] D.R. Heldman, "Encyclopedia of Agricultural, Food, and Biological Engineering", CRC Press, p. 188, 2003.
- [10] ISO. Atmospheric Icing of Structures. Standard ISO 12494:2001(E). Geneva, 2001
- [11] D. Bolduc, et al., "Field Measurement of Wind Turbine Icing", IWAIS XV, St-John's, 2013
- [12] R. Cattin, "Icing of Wind Turbines", Elforsk, Stockholm, 2012.